

Easy 3D Mapping for Indoor Navigation of Micro UAVs*

Henrik Schiøler, Luminita Totu, Anders la Cour-Harbo, John Josef Leth and Jesper Larsen

Department of Electronic Systems, Automation and Control, Aalborg University, Denmark

Keywords: UAS, 3D Mapping, Indoor Path Planning.

Abstract: Indoor operation of micro Unmanned Aerial Vehicles (UAV or UAS) is significantly simplified with the capability for indoor localization as well as a sufficiently precise 3D map of the facility. Creation of 3D maps based on the available architectural information should on the one hand provide a map of sufficient precision and on the other limit complexity to a manageable level. This paper presents a box based approach for easy generation of 3D maps to serve as the basis for indoor navigation of UAS. The basic building block employed is a 3D axis parallel box (APB). Unions of APBs constitute maps, which are by definition closed to basic set operations such as; union, intersection, set difference etc. The restriction to APBs is made in accordance with the tradeoff between simplicity and expressiveness, where real time requirements emphasize simplicity. The mapping approach is presented along with different approaches of selecting via points ensuring sufficiently efficient path planning and at the same time ensuring scalability by keeping complexity low. A proposition for *minimal* via point assignment is ensuring at least feasibility of path planning is presented. Feasibility is not proved formally. Instead results from a randomized *statistical proof* are given. 3D Mapping, via point assignment and calibration are all implemented in a stand alone software application. The application program provides, through a graphical user interface, the possibility to map indoor environments based on existing 2D floor maps.

1 INTRODUCTION

Robotic localization, route planning as well as the associated mapping have been investigated thoroughly through decades, where most efforts are made towards higher and eventually full autonomy (Martínez et al., 2013). Although impressive results have been achieved within *Simultaneous Localization and Mapping* (SLAM) such fully autonomous approaches still lack industrial adoption for highly efficient and reliable operation. A major difference between the underlying assumption behind the quest towards full autonomy and large scale industrial adoption is that industrial environments are most often well known and largely static, whereas unknown time varying environments are typically assumed to stress the capability for autonomy to the extreme.

Indoor operation has until recently been considered *GPS denied*. However, with the emergence of indoor positioning technologies such as (Theilgaard, 2016; de Velde, 2016) this assumption is to a large extent nullified. We consider the case for indoor in-

dustrial UAV operation based on the *Games On Track* (GoT) ultra sound based positioning technology. In that case on-board mapping could be performed with the aid of the global positioning system to reduce the inherent complexity of SLAM and in turn increase robustness to noise/disturbances and drifting inertial sensors. Although on-board ad hoc mapping is a viable opportunity, we argue the value of an initial map created prior to operation, providing a sufficiently precise basis for navigation within the main transportation highways in the facility. On top of and with aid of the initial map a finer ad hoc map may be created at a later stage using on-board sensors such as LIDAR and 3D camera.

The approach and tools presented in this paper constitute an attempt to bridge the gap between available 2D architectural information and operational 3D maps from which topological information for UAV route planning can be extracted. A comparable 2D approach is presented in (Boniardi et al., 2016), where hand drawn sketches provide the topological basis for mapping through SLAM. SLAM adds scaling and orientation to a diffeomorphic map between the sketched image and *real* rasterized image of the map domain. We find the sketching approach infeasible for 3D

*The UAWORLD project is partly funded by Innovation Fund Denmark

mapping but recognize the need for a user interface with the same high usability and in coherence with intuition. In (Lin et al., 2013) information is extracted from standardized *Building Information Models* (BIM) in *Industry Foundation Classes* (IFC) format to achieve floor constrained indoor path planning. In (Lin et al., 2013) floor areas are discretized into planar grids defining via points for paths. Although BIM provides an obvious input for indoor path planning, alternatives will be necessary for a significant time span due to the relatively low adoption of BIM even for new construction (Edirisinghe and London, 2015). We present a GUI with resemblance to 3D design tools such as Google SketchUp (Ske, 2017) but based on a restricted definition space for reduced complexity and support for 3D path planning. Our main modeling element is a so called Axes Parallel Box (APB), which makes our approach resemble that in (Yuan and Schneider, 2011), where boxes of (initially) fixed sizes are used as modeling building blocks through the *LEGO* approach. Whereas boxes in (Yuan and Schneider, 2011) are subsequently merged into larger elements in a *bottom-up* order we pursue a *top-down* approach, where large boxes are defined initially and subsequently partitioned into smaller elements of which some are appropriately deleted, i.e. the model is pruned. A formalism for combining APBs through symbolic set operations is presented, which could be seen as a subset of *Constructive Solid Geometry* (CSG) (Voelcker and Requicha, 1977). Confining the formalism to the APB subset of CSG reduces complexity allowing to give geometric properties explicitly and facilitating easy assignment of via points for path planning.

First the mapping formalism is introduced with examples. Next the GUI developed is presented through an example for the main test flight area of the UAWORLD project. Topological mapping is performed through the assignment of via points and associated *visibility graph*. We introduce the *feasibility problem* of assigning a sufficient set of via points to ensure reachability through via points followed by a proposition for its solution. In the absence of rigorous proofs for the proposition we present results from a randomized *statistical proof*, where a large sample of 3D maps are generated randomly to serve as counter example candidates. Next we give complexity considerations for the proposed mapping approach and compare with a grid based method for a real life example. Finally conclusions are given with a discussion of possible extensions and perspectives for future work.

2 AXES PARALLEL BOXES

As a basic descriptive element we use the APB, i.e. a 6-tuple $B = (x^1, x^2, y^1, y^2, z^1, z^2) \in \mathbb{R}^6$ interpreted geometrically as Cartesian coordinates for opposite box corners such that

$$\begin{aligned} x^1 &< x^2 \\ y^1 &< y^2 \\ z^1 &< z^2 \end{aligned} \quad (1)$$

Let \mathcal{B} denote the set of APBs. We define a *boxmap* M to be a finite union of boxes, i.e.

$$M = \cup_i^N \{B_i\}, \quad B_i \in \mathcal{B} \quad (2)$$

where $\{B_i\}$ is the singleton containing only the element B_i . As an example the boxmap R for a rectangular room could be given as

$$\begin{aligned} R = & \{floor\} \cup \{ceiling\} \cup \\ & \{easternwall\} \cup \{westernwall\} \cup \\ & \{northernwall\} \cup \{southernwall\} \end{aligned}$$

where each member of the union denotes an appropriate APB to be provided by the cartographer (user). In this case the user should then provide 6 times 6 coordinates. Let \mathcal{M} denote the set of boxmaps.

The example illustrates the use of APBs and boxmaps for describing physical structures within the facility. However, they may equally well describe imaginary blockings such as safety zones, where robot (UAV) access is prohibited.

3 BOXMAP ALGEBRA

Since boxmaps are constituted by sets of 6-tuples (APBs) they are by definition closed under set operations such as union, intersection and set difference. Adding boxmaps M_1 and M_2 is defined by set union, i.e.

$$\begin{aligned} + : \mathcal{M} \times \mathcal{M} &\rightarrow \mathcal{M} \\ M_1 + M_2 &= M_1 \cup M_2 \end{aligned} \quad (3)$$

Note how unions of boxmaps become practicable for merging or extending maps, e.g. in the case where maps are constructed on demand and neighboring rooms are added to the map in the order of creation.

We introduce an additional operation *box subtraction*: $- : \mathcal{B} \times \mathcal{B} \rightarrow \mathcal{M}$ such that for

$$\begin{aligned} A &= (x_A^1, x_A^2, y_A^1, y_A^2, z_A^1, z_A^2) \\ B &= (x_B^1, x_B^2, y_B^1, y_B^2, z_B^1, z_B^2) \end{aligned}$$

we define

$$\begin{aligned}
 A - B = & \{ (x_A^1, \min([x_A^2, x_B^1]), y_A^1, y_A^2, z_A^1, z_A^2), \\
 & (\max([x_A^1, x_B^2]), x_A^2, y_A^1, y_A^2, z_A^1, z_A^2), \\
 & (x_A^1, x_A^2, y_A^1, \min([y_A^2, y_B^1]), z_A^1, z_A^2), \\
 & (x_A^1, x_A^2, \max([y_A^1, y_B^2]), y_A^2, z_A^1, z_A^2), \\
 & (x_A^1, x_A^2, y_A^1, y_A^2, z_A^1, \min([z_A^2, z_B^1])), \\
 & (x_A^1, x_A^2, y_A^1, y_A^2, \max([z_A^1, z_B^2]), z_A^2) \}
 \end{aligned}$$

where APBs not fulfilling (1) are generally discarded from the result in order to avoid degenerate APBs representing empty or zero volume sets. The discard of degenerate APBs is implicitly assumed in the sequel. The definition of box subtraction can be generalized to boxmaps, i.e.

$$- : \mathcal{M} \times \mathcal{B} \rightarrow \mathcal{M} \quad (4)$$

$$M - B = \cup_{B_i \in M} (B_i - B) \quad (5)$$

Consider the room example above. With box subtraction the user can now provide coordinates for 2 APBs instead of previously 6, i.e.

$$R = \{outer\} - inner \quad (6)$$

where *outer* would be an APB comprising Cartesian coordinates for the outer wall corners and *inner* for interior corners. As a numerical example consider

$$\begin{aligned}
 outer &= (-1, 11, -1, 31, -1, 6) \\
 inner &= (0, 10, 0, 30, 0, 5)
 \end{aligned} \quad (7)$$

In this case

$$\begin{aligned}
 R = & \{(-1, 0, -1, 31, -1, 6), \text{ (western wall)} \\
 & (10, 11, -1, 31, -1, 6), \text{ (eastern wall)} \\
 & (-1, 11, -1, 0, -1, 6), \text{ (northern wall)} \\
 & (-1, 11, 30, 31, -1, 6), \text{ (southern wall)} \\
 & (-1, 11, -1, 31, -1, 0), \text{ (floor)} \\
 & (-1, 11, -1, 31, 5, 6) \} \text{ (ceiling)} \quad (8)
 \end{aligned}$$

which is given in a 3D depiction in figure 1 (without ceiling for illustrative purposes)

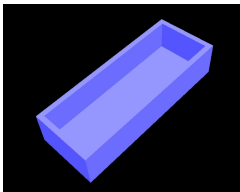


Figure 1: Room created from the subtraction of inner from outer boundaries.

For algorithmic purposes (explained in the sequel) we define a so called *almost disjoint box subtraction*,

i.e. if $A - B = \{D_1, D_2, D_3, D_4, D_5, D_6\}$ we define the *almost disjoint subtraction* $-_d$ by

$$\begin{aligned}
 A -_d B &= \{D_1, D_2 - D_1, D_3 - D_2 - D_1, \\
 & D_4 - D_3 - D_2 - D_1, \\
 & D_5 - D_4 - D_3 - D_2 - D_1, \\
 & D_6 - D_5 - D_4 - D_3 - D_2 - D_1\} \\
 &= \{Dd_i\} \quad (9)
 \end{aligned}$$

as well as for maps and APBs

$$-_d : \mathcal{M} \times \mathcal{B} \rightarrow \mathcal{M} \quad (10)$$

$$M -_d B = \cup_{B_i \in M} (B_i -_d B) \quad (11)$$

Although we have implicitly anticipated the formal geometric interpretation of APBs as subsets of \mathbb{R}^3 we have postponed a formal definition. For a geometric interpretation we define the membership relation between a point $(x, y, z) \in \mathbb{R}^3$ and an APB $B = (x^1, x^2, y^1, y^2, z^1, z^2)$ as

$$\begin{aligned}
 x \in B \iff & x^1 \leq x \leq x^2 \wedge \\
 & y^1 \leq y \leq y^2 \wedge \\
 & z^1 \leq z \leq z^2 \quad (12)
 \end{aligned}$$

which allows to define the coverage $|B|$ of B by

$$|B| = \{x \in \mathbb{R}^3 | x \in B\} \quad (13)$$

as well as the coverage of a boxmap $M = \{B_1, \dots, B_N\}$ by

$$|M| = \cup_{B_i \in M} |B_i| \quad (14)$$

With the definition of coverage, the following properties of the defined operations are easily established

$$\begin{aligned}
 |M + B| &= |M| \cup |B| \\
 |M - B| &= |M -_d B| = \overline{|M| \setminus |B|}
 \end{aligned} \quad (15)$$

where $\overline{\cdot}$ denotes set closure and \setminus denotes set difference in \mathbb{R}^3 . Also for $A -_d B = \{Dd_i\}$

$$\text{int}(|Dd_i| \cap |Dd_j|) = \emptyset \quad (16)$$

where $\text{int}(A)$ denotes interior of a set $A \subseteq \mathbb{R}^3$. We say that the APBs $\{Dd_j\}$ in (16) are *non-overlapping* or *almost disjoint*.

Since we use boxmaps M to define the space occupied by physical (or imaginary) obstructions (obstacles) the open space S is defined by

$$S = \overline{\mathbb{R}^3} \setminus |M|$$

and the flight space F as a subset thereof, i.e. $F \subseteq S$. For simplicity we assume F to be connected, i.e. mutual reachability between any two points of F . Formally this means that for any two points $o, d \in F$ a continuous curve $T : \mathbb{R} \rightarrow \mathbb{R}^3$ exists such that $T(t) \in F \forall t \in [0, 1]$ and at the same time $T(0) = o$ and $T(1) = d$. We say additionally that two points $o, d \in F$ are mutually *visible* if the straight line connecting them is entirely in F .

4 USER INPUT

Although the introduction of the box subtraction operation above is likely to release the user of significant burden, the numerical interface to 3D mapping seems unreasonably cumbersome for complex environment mapping. For that purpose we suggest a graphical user interface with an existing floor map as primary input. Maps may be in the possession of the user as architectural blueprints or e.g. as a ROS map captured through LIDAR scanning from a UGV (Unmanned Ground Vehicle).

4.1 Graphical User Interface

A *proof of concept* GUI, based on the *Irrlicht open source 3D engine* (Gebhardt, 2016), has been implemented. The first action performed by the user is to load floor map graphics, which is then shown as a background in the map design area as shown in figure 2 (a).

Exterior wall boundaries are then added as an APB by pointing mouse to upper left and lower right corners of the boundary. Vertical coordinates are provided through mouse wheel. Next, interior boundaries are given as an APB and subtracted to create surrounding walls.

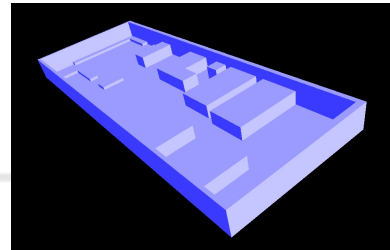
In the following mapping process the user will provide APBs for each box shaped obstacle inside the room and if necessary provide several APBs for obstacles far from box shape. An impression of the mapping process is shown in figure 2(a) with a 3D visualization in figure 2(b)

5 PATH PLANNING

A number of path planning approaches exist; such as gradient following with artificial potential fields (Horner and Healey, 2004), navigation functions created through the solution of the stationary heat equation (Connolly et al., 1990), which bears close resemblance to solving the shortest path problem for *all-to-one location*. Such approaches constitute feasible path planning back-ends to the 3D boxmap presented earlier. However, as described in (Scholer, 2012) any 3D shortest path in smooth environments is composed of an alternate sequence of straight lines and obstacle surface geodesics. We adopt this insight for path planning along with the restriction that any obstacle in a boxmap is indeed a polyhedron for which surface geodesics appear as sequences of straight lines. This in turn makes any path a connected sequence of



(a) 2D top view of interior obstacles included as Axes Parallel Boxes in map design area of prototype design application.



(b) 3D view of interior obstacles included as Axes Parallel Boxes.

Figure 2.

straight lines. A similar approach is taken in (Lozano-Pérez and Wesley, 1979) where obstacle avoidance and path planning is investigated for general polygons in the plane. From a computational point of view (Canny and Reif, 1987) proved that the 3D shortest path problem even for polyhedral obstacles is NP-hard, which calls for further reductions in complexity to allow scalability. Indeed in (Canny and Reif, 1987) the set of shortest paths are divided into classes with equivalent edge sequences. Within each class the shortest path problem is itself a non-convex real valued optimization problem.

5.1 Generation of Via Points

In the following we pursue the approach of (Lozano-Pérez and Wesley, 1979) in 3D, where the topology of the environment is given with a discrete set of via points as well as the *visibility graph* connecting them. At this point the question arises on how to identify a suitable set of via points. On the one hand the set of via points has to be sufficiently dense to allow a proper approximations of shortest paths and on the other hand to be of sufficiently low cardinality to not jeopardize scalability. Due to the real valued nature

of the problem, infinite density of via points on obstacle edges is needed to obtain optimality. We provide a user specified density on box edges to allow the user to make the tradeoff between precision and complexity. As opposed to the grid approach adopted by (Lin et al., 2013) defining via point to the open space, we confine via points to be associated only to obstacles. The reason for that is two-fold; since shortest paths are straight lines through open space, no via points are needed there and secondly the grid approach in (Lin et al., 2013) scales badly in higher dimensions.

Although precision is left as a design issue for the user, it seems valuable that our tool provides some assistance in avoiding *infeasible* via point sets. We say that a set of via points $V \subset F$ is *feasible* if, for each pair of mutually reachable points in the map, there is a path through via points. More precisely, if $o \in \mathbb{R}^3$ and $d \in \mathbb{R}^3$ are mutually reachable, then a subset $\{v_1, \dots, v_m\} \subseteq V$ exists so that the point pairs $\{(o, v_1), (v_1, v_2), \dots, (v_{m-1}, v_m), (v_m, d)\}$ are mutually visible. We say that points o and d are mutually reachable on V .

Feasibility of a set of via points V is ensured if all points in V are mutually reachable on V and for every point $o \in F$, $\exists v \in V$ such that o and v are mutually visible. Within computational geometry the problem of placing via points (guards) to make all other points visible from at least one via point, is equivalent to the so called *Fortress Problem* (O'Rourke, 1987), which has been predominantly treated in two dimensions, i.e. for polygons and in close connection with the related *Art Gallery Problem*. In (Viglietta, 2012) a 3D example (the *octoplex*) is given, where the Art Gallery Problem is unsolvable with via points confined to the vertices (corners) of the polyhedron. Similar to boxmap obstacles the octoplex is an orthogonal polyhedron. Since the 2D Fortress Problem can be reduced to the 2D Art Gallery Problem, it seems nearby to conjecture the 3D Fortress Problem unsolvable for via points confined to vertices. However the octoplex and its generalizations (multiplexes) are all *externally visible* from vertices, i.e. the Fortress Problem is solvable with via points confined to vertices for multiplexes.

For a boxmap comprising only non-overlapping APBs this is directly accomplished by assigning via points to all 8 corners of every APB. If some APBs are overlapping, the situation is more complicated. Overlapping APBs are handled through the definition of almost disjoint box subtraction. When an APB B is added to a boxmap M we shall instead of (3) apply the *almost disjoint box addition* in (17), i.e.

$$M' = M +_d B = M + B + (M -_d B) + (B -_d M) \quad (17)$$

which by definition is commutative. It is readily veri-

fied by inspection that

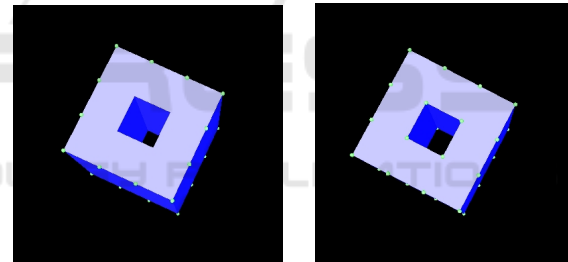
$$|M + B| = |M +_d B| = |M| \cup |B|$$

Next, if M includes a set of almost disjoint APBs $\{B_i\}$ so that $|M| = |\cup_i \{B_i\}|$ then M' includes a set of almost disjoint APBs $\{B'_i\}$ so that $|M'| = |\cup_i \{B'_i\}|$. We say that M and M' both have an *almost disjoint representation*. Thus, if a boxmap is constructed through consecutive applications of almost disjoint additions and subtractions, it contains at all times a set almost disjoint APBs occupying the same space. Every corner of these APBs will be assigned a via point leading to the result, that at least every vertex of the boxmap is equipped with a via point.

Consider the following map M

$$M = \{(0, 1, 0, 3, 0, 4), \\ (2, 3, 0, 3, 0, 4), \\ (0, 3, 0, 1, 0, 4), \\ (0, 3, 2, 3, 0, 4)\}$$

Assume each APB B_i in M is added according to (3) and equipped with via points at its corners. Then only the outside of the *tunnel* shown in figure 3(a) is equipped with via points, leaving the inside of the tunnel *invisible*.



(c) Tunnel with exterior via points and *invisible* positions inside (d) Tunnel with via points on inner edges and *visible* positions inside

Figure 3.

If on the other hand each APB B_i in M is added according to (17) via points are also assigned to the inner corners of the tunnel, rendering the inside of the tunnel visible as shown in figure 3(b).

5.2 Feasibility Proposition and Statistical Proof

We conjecture the feasibility of the presented method, i.e. boxmaps constructed through consecutive applications of (17) and via points are assigned to all corners of all APB's in the map. The restriction to *almost disjoint box addition* (17) represents no loss of generality, since every boxmap $M = \{B_i\}$ can be recomputed recursively through (17) yielding the desired result.

Some effort has been put into the formal proof of the presented proposition without success. Thus, in the absence of formal proof a statistical proof has been devised as presented below.

- for $i=1:N$
 - Generate random path P connecting end points O and D
 - Generate random boxmap $M = \{B_1, \dots, B_L\}$ not intersecting P (through consecutive applications of almost disjoint addition)
 - Assign viapoints $\{v_p\}$ to all corners of all APBs in M
 - Compute visibility graph G for $\{O, D, \{v_p\}\}$ and M
 - Compute path $P' = O, v_{k_1}, \dots, v_{k_n}, D$ in G

The origin $O = (0,0,0)$ is fixed through all iterations $1, \dots, N$. For each iteration the random path is specified through a sequence of points $O = p_1, \dots, p_{Q+1} = D$ defined as a random walk. The boxmap $M = B_1, \dots, B_K$ is generated through an *accept/reject* strategy. The accept/reject strategy discards boxes intersecting line segments (p_{i+1}, p_i) such that a path connecting O and D is guaranteed by design. The procedure continues until the specified number L of APBs are accepted. One representative sample is shown in figure (4).

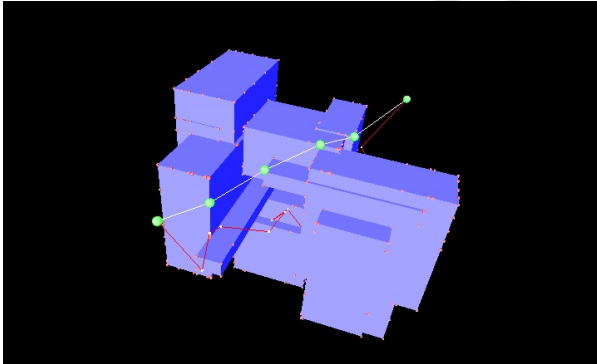


Figure 4: Randomly generated path, boxmap and path through via points. Random path P is shown as red lines, the path through via points P' shown in white lines and complete set of via points shown as red boxes.

For every iteration the *non-existence* of the path P' constitutes a counter example for the presented proposition regarding the feasibility of via point assignment. So far P' has existed for $N = 50.000$ consecutive iterations with $Q = 10$ and $K = 20$.

5.3 Flight Altitude Levels

Additionally a finite number of preferred altitude flight levels $L = \{l_1, \dots, l_N\}$ are defined. For each APB we define path via points on the intersection between the APB surface and each flight level, i.e. for $B = (x^1, x^2, y^1, y^2, z^1, z^2)$ we define B_∞ by

$$B_\infty = (x^1, x^2, y^1, y^2, -\infty, \infty) \quad (18)$$

$$vp \in B_\infty \cap \{(x, y, z) | z \in L\} \quad (19)$$

where vp is a via point. To allow for vertical climb and descent, we provide additional via points by using (in (19)) an extension B_∞ of the APB extended vertically to cover all flight levels. On the intersection via points are defined at least on edges but may be set by a maximum distance to encircle the APB in each flight level. A 3D impression of an APB with via points in 3 flight levels is shown in figure 5

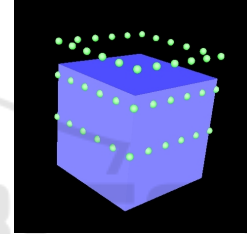


Figure 5: APB $(0,10,0,10,0,10)$ with via points defined for flight levels $(7,9,12)$ at a distance 2.

5.4 Reduction of Via Points

As such any obstacle in a boxmap generates its own via points necessary for avoiding it. Some APBs can however appropriately be excluded from generating via points; namely walls without openings as well as floors and ceilings. A 3D image illustrating a boxmap with via points only on *inner* obstacles is shown in figure 6.

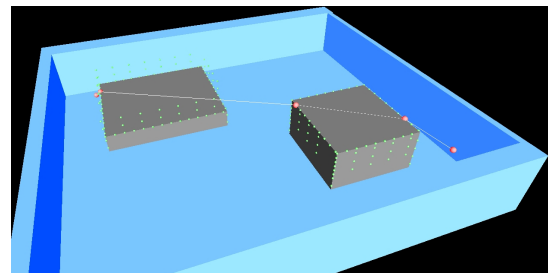
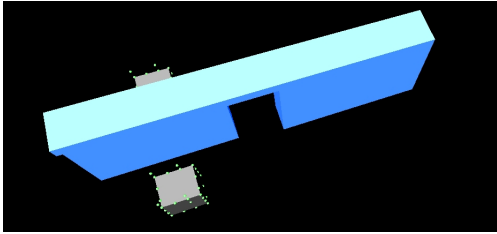


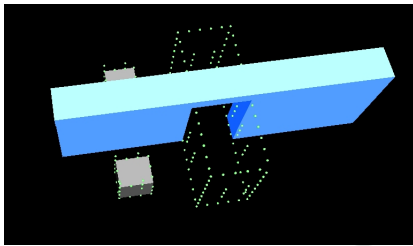
Figure 6: Boxmap with via points only on obstacles and flight path.

Excluding part of the boxmap from generating via points provides a welcomed opportunity for reducing

the complexity of the map and in turn supporting scalability. However, it may on the other hand jeopardize feasibility. Consider the case where two rooms are connected by wall opening (door/window) and the wall does not itself generate via point. Such a situation is depicted in figure 6(a).



(a) Infeasible via point set for separating wall.



(b) Feasible via point set for separating wall.

Figure 6.

To counteract this problem, we provide the opportunity to let subtracted boxes such as wall openings generate via points. The example from 6 can be remedied by allowing the door opening to generate via points as shown in figure 6(b).

6 OBSTACLE DILATION

The exposition so far, considered neither the physical dimensions of the vehicle itself nor the need for safety zones around physical obstacles. Both concerns are met through the definition of δ -padding of APBs, i.e. for $B = (x^1, x^2, y^1, y^2, z^1, z^2)$

$$\begin{aligned} \cdot^\delta &: \mathcal{B} \rightarrow \mathcal{B} \\ B^\delta & \\ &= \\ (x^1 &- \delta, x^2 + \delta, y^1 - \delta, y^2 + \delta, z^1 - \delta, z^2 + \delta) \end{aligned} \quad (20)$$

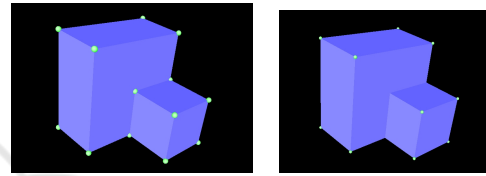
δ -padding, as presented, is a rather crude approach to dilation, which in fact presumes cubic physical dimensions $(2\delta, 2\delta, 2\delta)$ of the vehicle. It is however straight forward to extend the definition to vector valued δ , presuming vehicle dimensions $(2\delta_x, 2\delta_y, 2\delta_z)$.

This however does not directly take into account attitude changes of the vehicle. We assume attitude changes are predominantly around the z -axis (*yaw*) and set $\delta = (\max\{\delta_x, \delta_y\}, \max\{\delta_x, \delta_y\}, \delta_z)$.

δ -padding needs to be considered in relation to feasibility of via points. With the definition of almost disjoint box operations given above, we may assume that all obstacles have almost disjoint representations. Without δ -padding paths exist between APBs with overlapping faces. Consider an example where $M = A + B$ and

$$\begin{aligned} A &= (0, 1, 0, 1, 0, 1) \\ B &= (1, 2, 0, 2, 0, 2) \end{aligned}$$

with via points on box corners as illustrated in figure 7(a)



(c) Boxmap without δ -padding. (d) Boxmap with δ -padding on every APB.

Figure 7.

Without δ -padding via points $v_1 = (1, 1, 1)$ and $v_2 = (1, 0, 0)$ would be mutually visible even though there is *no room* between A and B . On the other hand, with δ -padding $v_1^\delta = (1 + \delta, 1 + \delta, 1 + \delta)$ belongs to the interior of $|B^\delta|$, which in turn jeopardizes the feasibility of via point assignment as illustrated in figure 7(b).

We introduce the almost disjoint summation \cdot^δ recursively, i.e. for $M = \{B_1, \dots, B_N\}$ and $\Gamma: \mathcal{B} \rightarrow \mathcal{B}$

$$\begin{aligned} M_1 &= \Gamma(B_1) \\ M_i &= M_{i-1} +_d \Gamma(B_i) \\ \sum_{B_i \in M} \Gamma(B_i) &= M_N \end{aligned} \quad (21)$$

With the definition of almost disjoint summation we may extend the definition of δ -padding to boxmaps. We define *almost disjoint* δ -padding \cdot^δ : for boxmaps by

$$\begin{aligned} \cdot^\delta &: \mathcal{M} \rightarrow \mathcal{M} \\ M^\delta &= \sum_{B_i \in M} B_i^\delta \end{aligned} \quad (22)$$

The example boxmap with almost disjoint δ -padding is shown in figure 8. Since the almost disjoint δ -padded boxmap in figure 8 includes both A^δ and B^δ no paths exist in between the touching faces of APBs

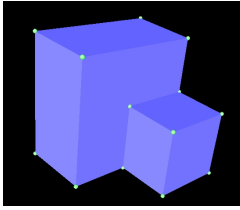


Figure 8: Boxmap with almost disjoint δ -padding.

A and B . On the other hand, it also includes both $A^\delta -_d B^\delta$ and $B^\delta -_d A^\delta$, which ensures via points on all corners of $|M|$.

7 COMPLEXITY CONSIDERATIONS

The suggested method generates complexities in different stages. Assume a boxmap $M = \{B_1, \dots, B_M\}$ is defined by the user through the graphical user interface. For via point assignment an almost disjoint representation $\{A_1, \dots, A_L\}$ needs to be computed, where potentially $L \gg M$. The complementary $(B_i^0)^c$ of any APB B_i^0 has a finite almost disjoint representation $\{B_i^1, \dots, B_i^6\}$. Now consider intersections such as $C = \bigcap_{j=1..M} |B_j^{k_j}|$, then an APB A exists such that $|A| = C$. Denote by C the set of such APBs. There are at most 8^M such intersections, which are all disjoint and constitute a partition of \mathbb{R}^3 . For any APB B_i in M we have

$$|B_i| = \bigcup_{p=0..7} \bigcap_{j<i} |B_j^{k_j}| \cap |B_i^p| \cap \bigcap_{j>i} |B_j^{k_j}| \quad (23)$$

Thus, an almost disjoint representation entirely in C of M exists. Since $\#C = 8^M$, we have $L \leq 8^M$. This number is however extremely large compared to realistic situations. For the M-tech lab case introduced above we have $M = 22$ and $L = 44$, whereas $8^M = 7.4E19$.

We assign via points to all corners of APBs in the disjoint representation $\{A_1, \dots, A_L\}$ as well as all edges and flight levels of APBs in $\{B_1, \dots, B_M\}$ with some distance δ . This amounts to $V = 8L + 12M \lceil \frac{D_B}{\delta} \rceil + ML_f 4 \frac{D_B}{\delta}$ via points, where D_B is an upper bound on APB dimension and L_f is the number of predefined flight levels. For the M-tech lab case we set $D_B = 10$, $\delta = 0.5$ and $L_f = 3$ which amounts to $V = 10912$. The M-tech lab covers $40 \times 14 \times 9 m^3$ such that covering it with via points in a regular grid of distance δ amounts to 37169 via points (in open space). However the bounds applied are overly pessimistic as results from mapping the M-tech lab demonstrates. After pruning away corners entirely in the interior of APBs, we get 336 via points on APB corners, 1164

via points on APB edges and finally 1230 for 3 flight levels amounting to 2730 via points. Creating the visibility graph is linear in the product $V^2 \times M$ or in this case $2730^2 * 22 = 163.963.800$. This can be done in 400 seconds on an Intel Quad Core Atom processor running 1.33 Ghz. Although significant, the computation of the visibility graph is a *one time endeavor*, whereas including a new origin-destination pair in the visibility graph is done in 59ms. We assume computing the visibility graph for regular grids is of lower complexity due to simple neighbor relationships and may be done during path finding. Path finding either by the Dijkstra- (Dijkstra, 1959) or the A^* -algorithm (Hart et al., 1968) is known to scale quadratically with the size of the graph. Since we have not implemented path finding for regular grids we compare the above numbers, i.e. 37169 via points for a regular grid and 2730 for the proposed method. Applying a quadratic scale we obtain a complexity advantage of the proposed method over regular grids of approximately 185 times. A number of paths in the visibility graph for the M-tech map are conducted with execution times around 100ms.

8 CONCLUSION

The paper presents an approach to easy (user-friendly) 3D mapping of interior environments for indoor UAV operations. The basic mapping element is the Axes Parallel Box (APB) for which algebraic operations are defined and made applicable to the user to allow both *additive* mapping, where obstacles are added consecutively to the map and *subtractive*, where openings such as doors and windows can be inserted. A SW application is developed, providing a Graphical User Interface allowing the user to construct a 3D map based on available 2D floor maps. Floor maps may appear either in the shape of an architectural blue print or, as exemplified in the paper, a ROS map acquired through LIDAR measurements from an UGV. A framework for topological mapping is presented, where a finite set of via points is defined, such that every flight path is defined as a sequence of via points. A minimal requirement *feasibility* is defined as the guarantee, that for every mutually reachable pair of via points there is a path through via points. A procedure to guarantee feasibility is presented along with a statistical proof of the correctness of the procedure.

Possible extensions are discussed for interiors with a major presence of non axes-parallel structural elements. It is suggested to confine such extensions to be overall additive to maintain a reduced complex-

ity. Complexity is considered in comparison with a regular grid approach and for a benchmark example. Results point unambiguously in favor of the proposed procedure. A procedure for aligning map coordinates with the coordinates of an indoor positioning systems is implemented in the developed SW application but left out of this presentation for brevity.

We find the presented methodology to be a useful candidate approach for user-friendly 3D mapping of UAV flight spaces both as a stand-alone tool, but also in combination with e.g. SLAM based solutions. One could foresee our solution to define the initial map to be subsequently refined over time with information from a SLAM procedure. Such approaches along with the presented extension possibilities of the mapping procedure outline directions for future research. This along with formal proofs of conjectured feasibility results which are only supported by convincing statistical evidence in this paper. Formal feasibility proofs would indeed be an independent result within computational geometry.

REFERENCES

- (2017). SketchUp. <https://www.sketchup.com/>. [Online; accessed 28-February-2017].
- Boniardi, F., Valada, A., Burgard, W., and Tipaldi, G. D. (2016). Autonomous indoor robot navigation using a sketch interface for drawing maps and routes. In *2016 IEEE International Conference on Robotics and Automation (ICRA)*, pages 2896–2901.
- Canny, J. and Reif, J. (1987). New lower bound techniques for robot motion planning problems. pages 49–60.
- Connolly, C. I., Burns, J. B., and Weiss, R. (1990). Path planning using laplace’s equation. In *In Proceedings of the 1990 IEEE International Conference on Robotics and Automation*, pages 2102–2106.
- de Velde, S. V. (2016). Pozyx-Accurate positioning. <https://www.pozyx.io/>. [Online; accessed 08-July-2016].
- Dijkstra, E. W. (1959). A note on two problems in connexion with graphs. *Numer. Math.*, 1(1):269–271.
- Edirisinghe, R. and London, K. (2015). Comparative analysis of international and national level bim standardization efforts and bim adoption. In *Proceedings of the 32nd International Conference of CIB W78, CIB W78*, pages 149–158.
- Gebhardt, N. (2016). Welcome to the Irrlicht Engine. <http://irrlicht.sourceforge.net/>. [Online; accessed 08-July-2016].
- Hart, P. E., Nilsson, N. J., and Raphael, B. (1968). A formal basis for the heuristic determination of minimum cost paths. *IEEE Transactions on Systems, Science, and Cybernetics*, SSC-4(2):100–107.
- Horner, D. P. and Healey, A. J. (2004). Use of artificial potential fields for uav guidance and optimization of wlan communications. In *Autonomous Underwater Vehicles, 2004 IEEE/OES*, pages 88–95.
- Lin, Y.-H., Liu, Y.-S., Gao, G., Han, X.-G., Lai, C.-Y., and Gu, M. (2013). The ifc-based path planning for 3d indoor spaces. *Advanced Engineering Informatics*, 27(2):189 – 205.
- Lozano-Pérez, T. and Wesley, M. A. (1979). An algorithm for planning collision-free paths among polyhedral obstacles. *Commun. ACM*, 22(10):560–570.
- Martínez, C., Mondragón, I. F., Campoy, P., Sánchez-López, J. L., and Olivares-Méndez, M. A. (2013). A hierarchical tracking strategy for vision-based applications on-board uavs. *Journal of Intelligent & Robotic Systems*, 72(3):517–539.
- O’Rourke, J. (1987). *Art Gallery Theorems and Algorithms*. Oxford University Press, Inc., New York, NY, USA.
- Scholer, F. (2012). *3D Path Planning for Autonomous Aerial Vehicles in Constrained Spaces*. PhD thesis.
- Theilgaard, N. B. (2016). Model Railroad without wires. <http://www.gamesontrack.dk/>. [Online; accessed 08-July-2016].
- Viglietta, G. (2012). Guarding and searching polyhedra. *CoRR*, abs/1211.2483.
- Voelcker, H. B. and Requicha, A. A. G. (1977). Geometric modeling of mechanical parts and processes. *Computer*, 10(12):48–57.
- Yuan, W. and Schneider, M. (2011). *3D Indoor Route Planning for Arbitrary-Shape Objects*, pages 120–131. Springer Berlin Heidelberg, Berlin, Heidelberg.